J.K.A.U.: Mar. Sci., **Vol. 2**, pp. 33-48 (1411 A.H./1991 A.D.)

Gravity Implications of Qusier-Mersa Alam Offshore Area, Red Sea, Egypt

M.B. AWAD, Y.I. EL-ABD and E.A. EL-HAJ
National Inst. of Oceanography, Alexandria, Egypt;
Faculty of Science, University of Alexandria; and
WEPCO Company, Alexandria, Egypt.

ABSTRACT. The aim of the present study is to evaluate the sub-bottom geological setting of Qusier-Mersa Alam offshore area in relation to possible hydrocarbon entrapment. Marine gravity, as well as bathymetric data in addition to one seismic and two well logs have been used for this evaluation.

One subsurface geological map for shallow structures and two NE-SW geological models, are constructed to illustrate the tentative picture of the basement and its overlying sediments.

The results show a clysmic NW-SE major trend of faults dissect the continental and/or Oceanic Crust and form an alternation of grabens and horsts. A minor NE-SW trend of faults is also observed. The deep seated structures are framed out into a great monoclinal feature dipping westward with a rapid thinning of the continental crusts. This study points out the possibility of hydrocarbon resources occurrence within the wedges and truncations of the Post Miocene interfaces.

Introduction

Quseir-Mersa Alam offshore area lies on the northern part of the Red Sea (Fig. 1). It is confined between latitudes 25°N and 26°N and longitudes 34°E and 35°30′E. The bathymetric data show that the sea water depth, in the area, is between 100 m (at the west) and 1000 m (at the extreme eastern border).

Tectonically, the Red Sea development is a result of the relative motion of the Arabian-African plates (Darke and Girdler 1964; Lowell and Genik 1972).

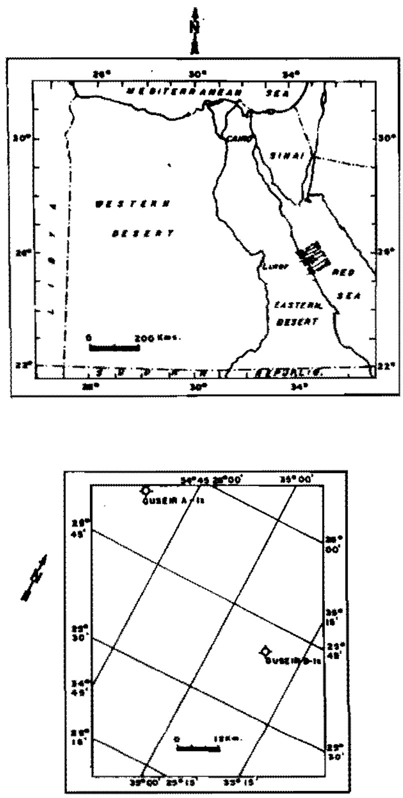

Fig. 1. Location map for Quseir, Mersa Alam, Red Sea.

Area under study.

Moreover, Rosser (1975), based on magnetic anomalies, proved that sea floor spreading contributes its development. Recently, Kabbani (1970), pointed out that the origin of the Red Sea basin is a result of different phases of arching, thinning, stretching and intensive faulting (due to continuous rifting system). However, it is important to mention that: (i) the tectonic activities continued intermittently until the present time, as indicated by the presence of hot brines in the Red Sea (Barker and Schoell 1972). (ii) regional major faults that trend NNW-SSE are present at the Red Sea graben shoulders. (iii) major (NNE-SSW) cross-faults are clear on landsat images of Wadi Araba and its surroundings.

Available Data and Methods of Interpretation

The available data include a Bouguer gravity map (Fig. 2), a NE-SW Seismic section (Fig. 3), and two composite logs of Qusier B-1X and B-2X exploratory wells (Fig. 4) all provided by the WEPCO company

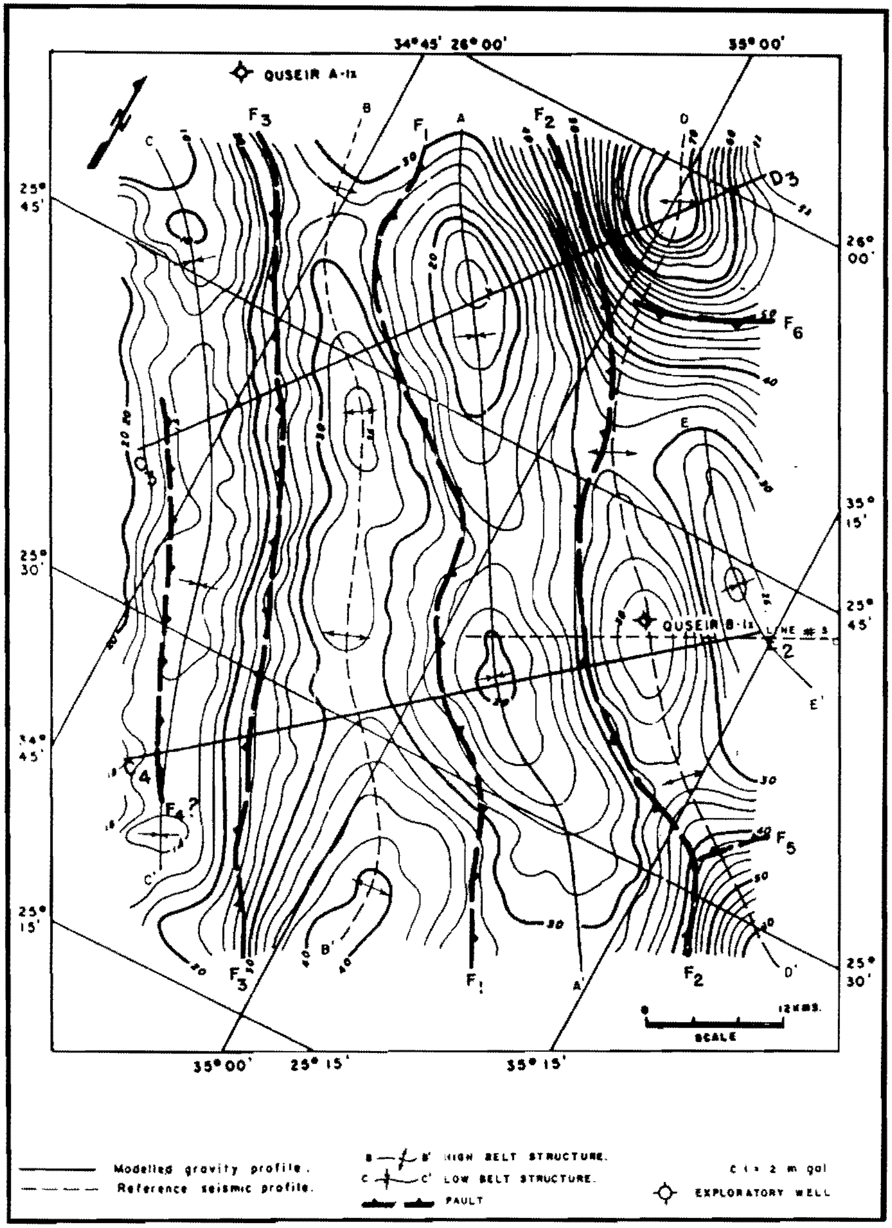

FIG. 2. Qualitative interpretation of Bouguer gravity map.

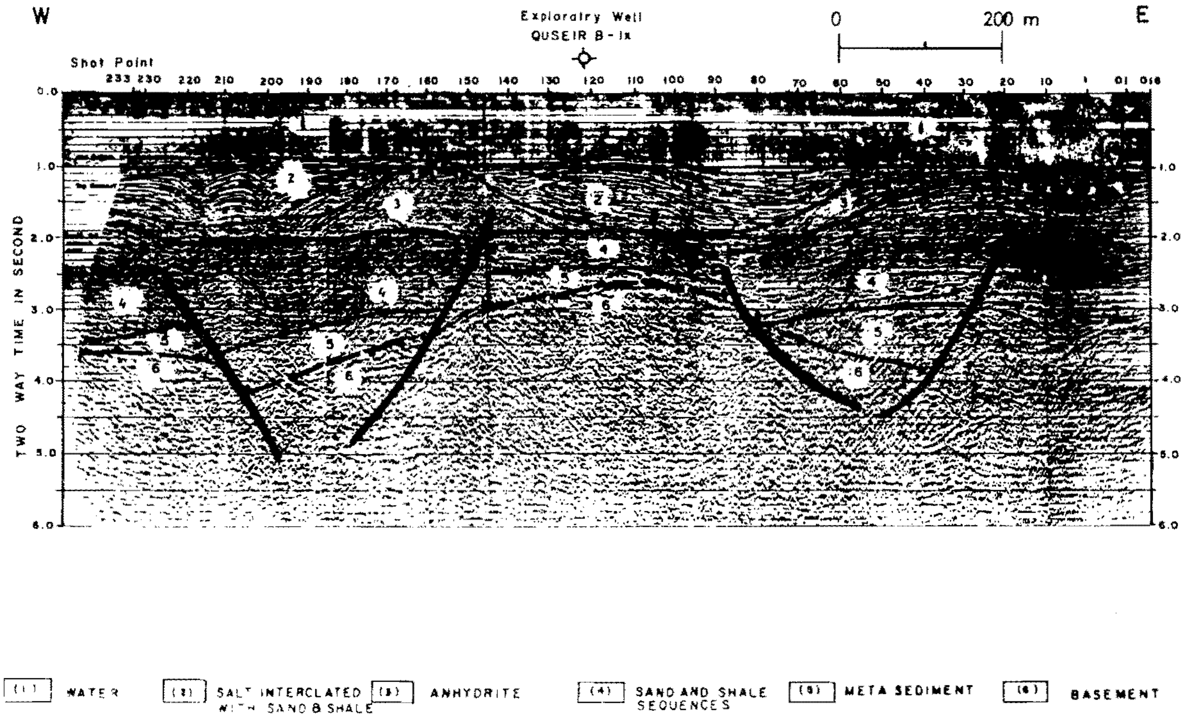

FIG. 3. Reference seismic section(s).

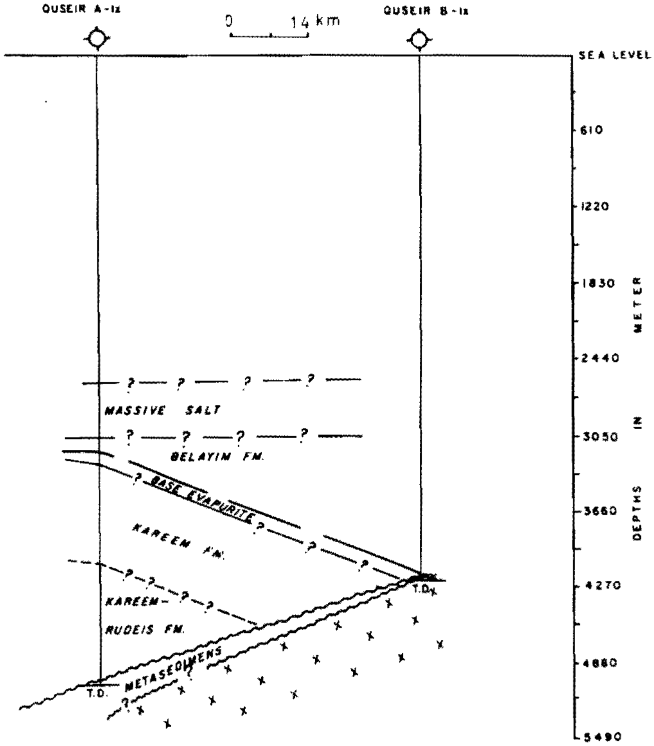

FIG. 4. Tentative picture of the subbottom geology along a profile between Quseir A-1X and B-1X exploratory wells.

Bouguer Data Analysis

About 1500 gravity data points, at the corners of 2 km side mesh squares, were picked from the Bouguer gravity map. The obtained data were subjected to different filter analysis techniques (for grid spacings: 2, 4, 6 and 8 kms). The application of least square technique for low order polynomial (Davis 1973) was tested and was found to be the best expression for the regional trend in the study area. The resulting regional and residual maps are shown in Fig. 5 and 6, respectively.

The second vertical derivative was calculated by using the Rosenbach's technique (1953). The resulted derivative anomaly map, for grid spacing 4 kms, is shown in Fig. 7. From the analysis of the previously obtained maps, a compiled shallow structural map (Fig. 8) was constructed.

Model Studies

The modelling technique is facilitated by using the computer program introduced by Talwani *et al.* (1964), developed by Nagy (1974) and modified by Ajakaiye and

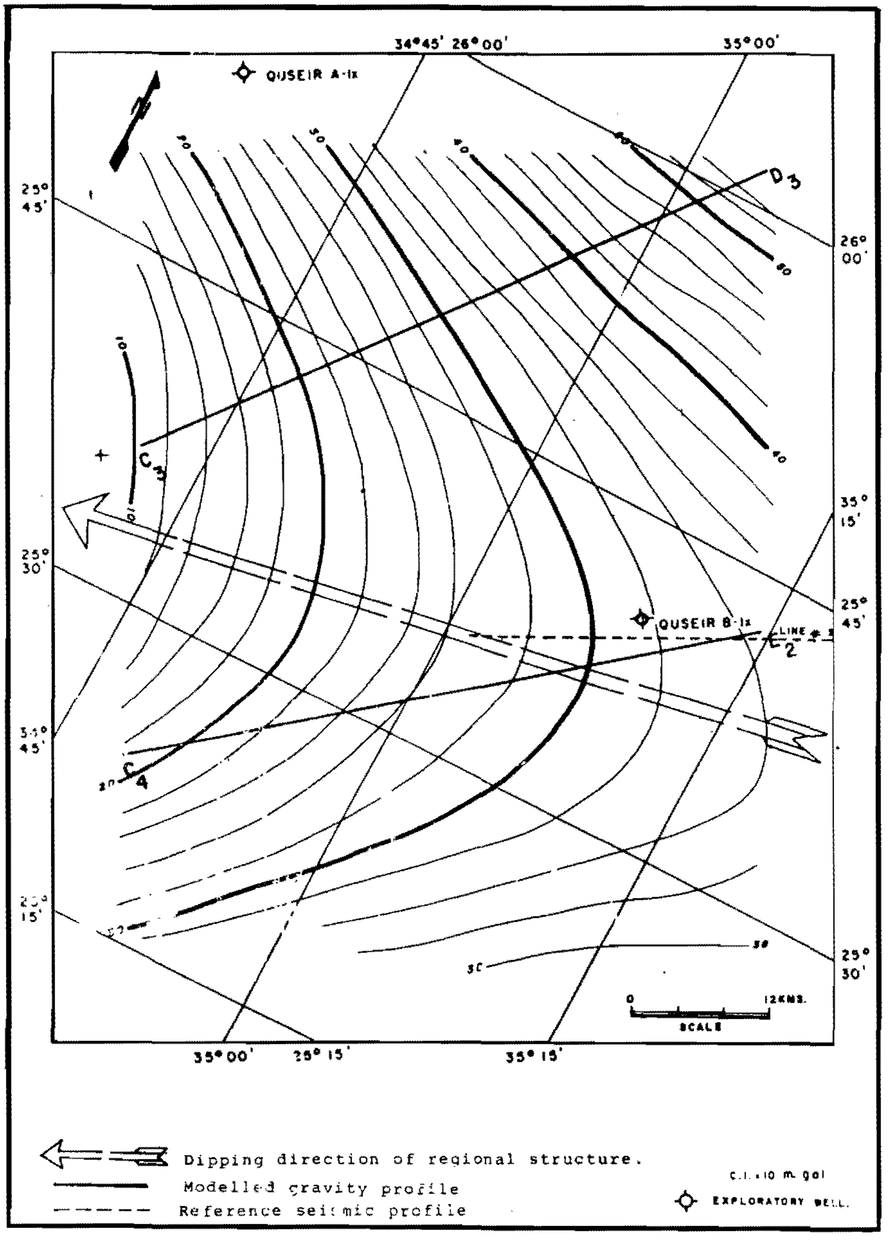

FIG. 5. Estimated regional trend by least squares fitting of low order polynomial.

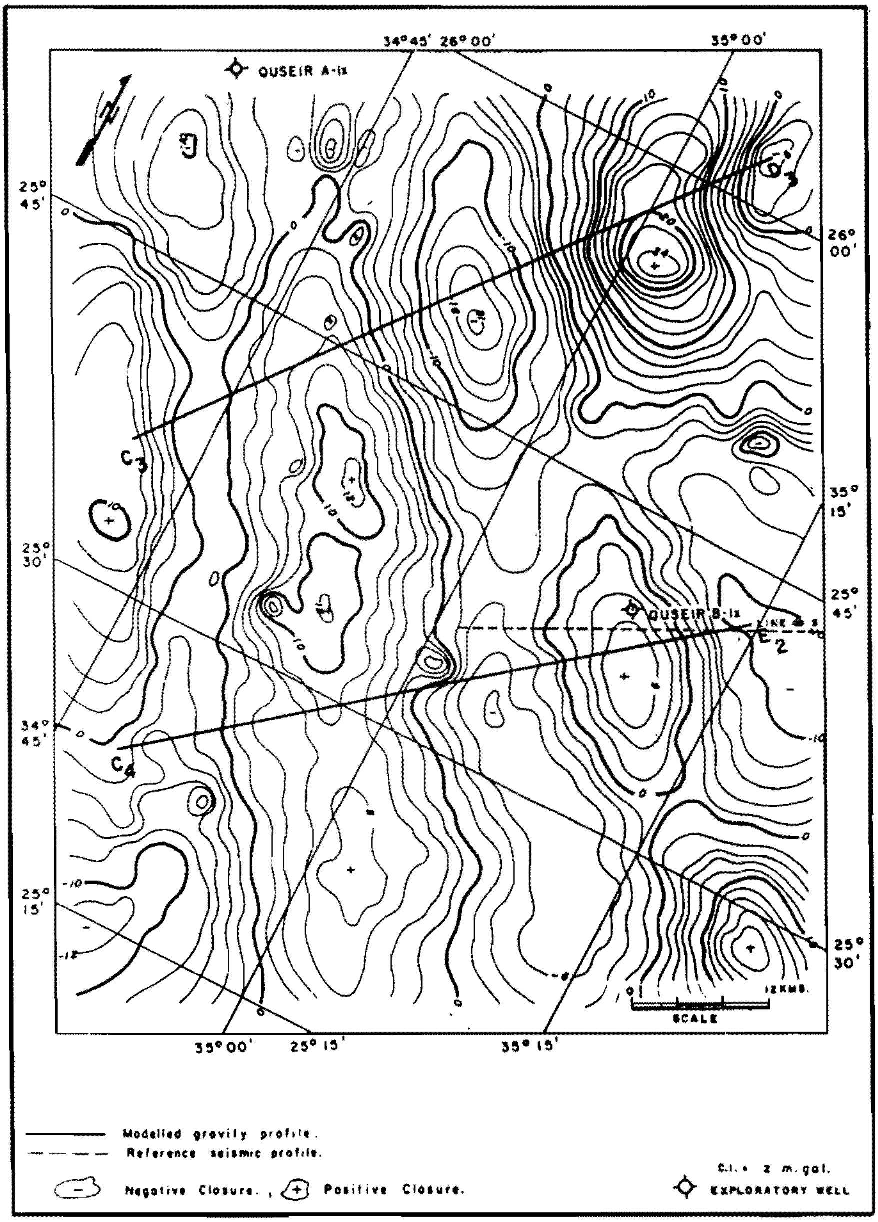

FIG. 6. Residual anomaly map by least squares filtering.

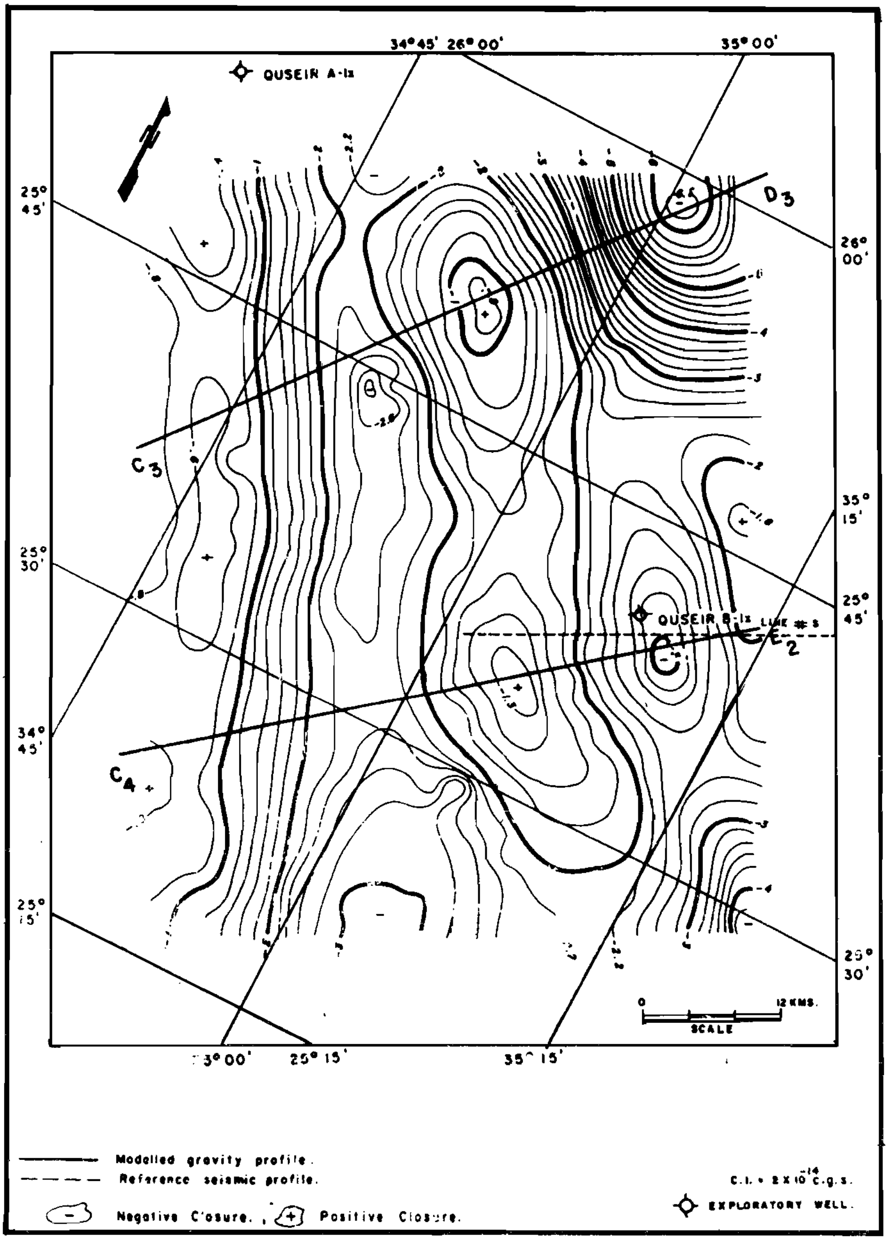

FIG. 7. Computed second vertical derivatives by Rosenbach's method (4 km spacing).

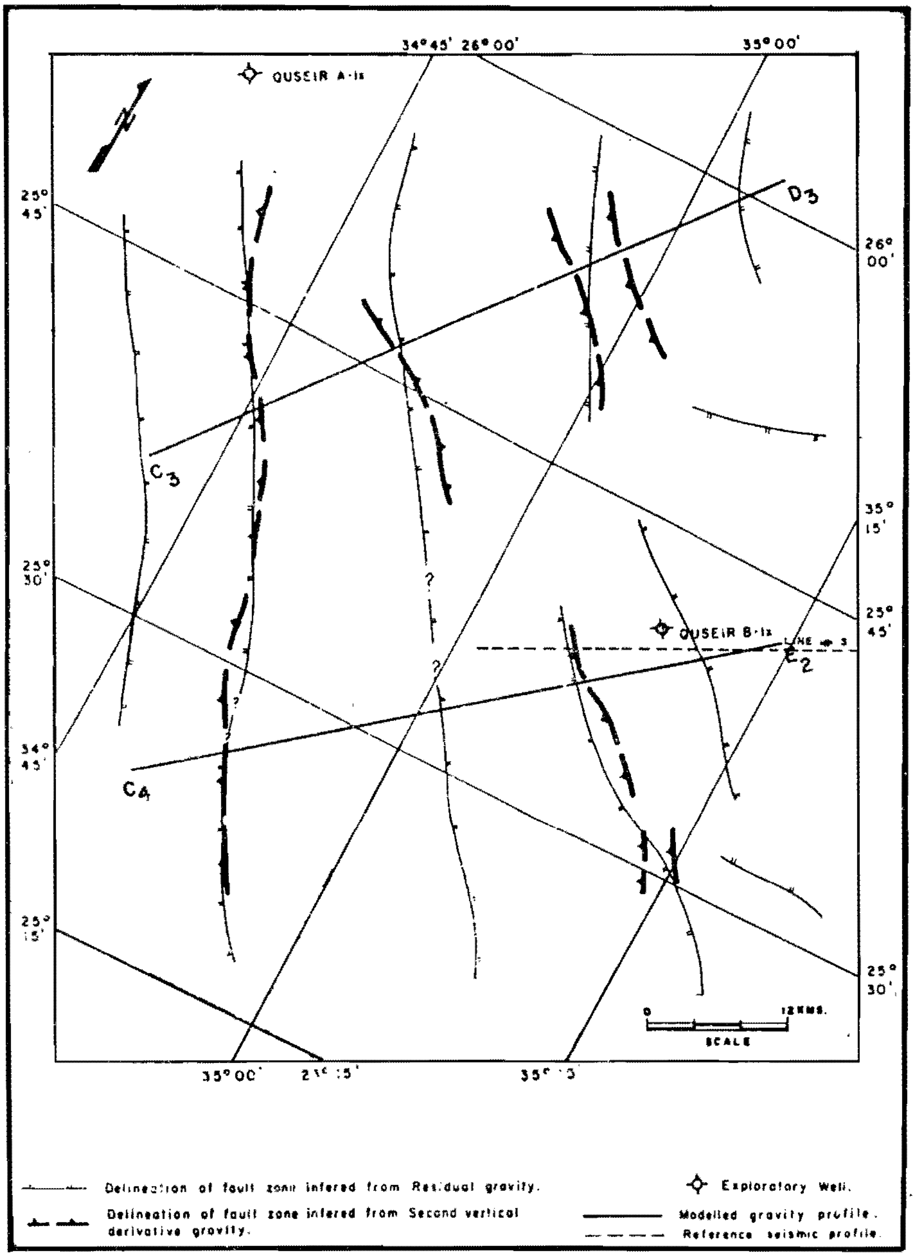

FIG. 8. Compiled shallow structural map revealed from the qualitative interpretation of residual and second vertical derivative of gravity potential.

Awad (1982). The basic theory starts by assuming an n-sided polygon to approximate the outline of the vertical section of a two-dimensional body (Fig. 9). The gravity effect of this section is equal to the line integral around the perimeter (Hubbert 1948) and is represented by the equation :

$$g = 2\,G\,\rho \oint z\,d\,\theta$$

This equation was introduced by Telford *et al.* (1976) in the form :

$$g = 2\,G\,\rho \sum_{i=1}^{n} D_i$$

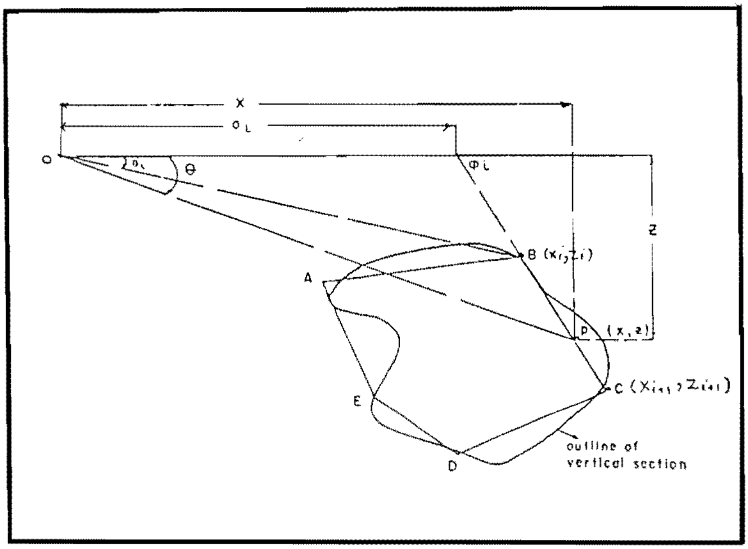

FIG. 9. Diagram showing the principle of two-dimensional modeling for gravity interpretation (after Grant and West 1965).

where D_i is the line integral due to the *i th* side of the polygon dipping by an angle ϕ_i, extended between the two corners *i*, *i* + 1 and of coordinates (X_i, Z_i), (X_{i+1}, Z_{i+1}) respectively.

$$\therefore D_i = a_i \sin\phi_i \cos\phi_i \, ((\theta_i - \theta_{i+1}) + \tan\theta_i \log\left(\frac{\cos\theta_i\ (\tan\theta_i - \tan\theta_i)}{\cos\theta_{i+1}\ (\tan\theta_{i+1} - \tan\phi_i)}\right))$$

where :

$$a_i = X_{i+1} - Z_{i+1} \cos\phi_i$$

$$\theta_i = \tan^{-1} (Z_i / X_i) .$$

$$\text{and } \phi_i = \tan^{-1} \left(\frac{Z_{i+1} - Z_i}{X_{i+1} - X_i}\right)$$

For the best model postulation, the following are considered :

a. Geological boundaries, interfaces between different formations, average dips of different beds and fault planes with their relative displacements.,

b. Formation densities have to be available with the value of 1.03×10^3 kg m^{-3} is taken for sea water density. The exploratory well Qusier B1x is taken as a reference considering that the basement is of gabbroic type (oceanic crust) of density 2.825×10^3 kg m^{-3}.

c. Bott and Smith (1958) proposed a formula for calculating the maximum depth of basement structure which is used as a guide in modelling postulation.

Two profiles, C_3 D_3 and C_4 E_2, running across the perpendicular to the predominant anomalies of the Bouguer and residual anomaly maps (Fig. 2 and 6) were selected. For each profile, a certain stratigraphic geological model was postulated, the coordinates of its corners were picked up and fed to the computer. The theoretical anomaly profile is computed several times for each model. Each time, different density contrasts, positions and shapes of stratigraphic bodies, are used.

Results and Discussion

Concerning the Bouguer Map

Referring to the composite log section (Fig. 4), inspection of the Bouguer map (Fig. 2) shows that :

a. The study area is affected by given gravity belts, (AA', BB', DD', and EE') of NW-SE trend parallel to the clysmic trend of the Red Sea. These belts comprise many local anomalies of elliptic shape.

b. The area is dissected by a set of NW-SE trending faults, as indicated by the maximum gradient zones (> 2.5 mgal/km) separating the gravity belts.

c. The major negative belt AA', is of about 12 mgal maximum relief and 190 km^2. It could be recognized as a synclinal feature, bounded by two faults (F_1 F_1 and F_2 F_2) from its eastern and western sides, respectively.

d. The positive belts DD' and BB' bound AA' from the east and west respectively. DD' covers an area of about 200 km^2 and comprises the highest relief (28 mgal) throughout the extreme NE and SE of the study area. BB' is about 12 mgal maximum relief and covers about 750 km^2.

e. The negative belt CC' lies to the west of BB' at the western border of the area and has a maximum relief of about 8 mgal and covers an area of about 680 km^2. It is found that the two belts CC' and BB' are separated by a fault zone F_3 F_3'. Moreover, the general tendency, behaviour, and flowage of contour lines, defining the belt CC' may suggest the existence of another fault F_4 F_4'.

f. The belt EE' lies at the eastern border of the map area. It is assumed that the two belts EE' and DD' are separated by the two faults F_5 F_5' and F_6 F_6' perpendicular to the Red Sea trend.

g. The dominating fault system F_1, F_2, F_3 and F_4 suggest that the study area is structurally composed of successive horsts and grabens.

h. The inferred fault zones F_5 and F_6 are assumed to be of shallows origin.

Concerning the Regional, Residual and Second Vertical Derivative Gravity Maps

As shown in Fig. 5, the regional gravity map describes an increase of gravity field from SW (10.0 mgal) to NE (54.0 mgal). This behaviour of the contour lines is probably due to a huge monoclinal feature of an axis dipping E-W. The attitude of the regional gravity may show the general configuration of the basement complex.

The residual anomaly map (Fig. 6) shows a consistency of the same alternation +ve and – ve anomaly belts (which are inspected before from the Bougeur map) associated with some changes in areal extent, relief, and gradient sharpness. Accordingly it is believed that :

a. These belts are of both deep on shallow origins *i.e.* corresponding causative elements are affecting both basement and the overlying sedimentary section.

b. The main causative gravity anomalies are of structural origin rather than an excessive lithologic variation within the sedimentary section.

c. The contribution of structural and lithological causative elements may be a third source of the gravity anomalies.

The second vertical derivative map (Fig. 7) shows all of the fault zones and the inferred alternation of grabens and horsts inspected from the Bouguer and residual map.

Concerning the Compiled Structural Map

From the compiled shallow structural map (Fig. 8), it is remarked that :

a. The NW-SE trend is dominating all over the area. This may suggest that the whole sedimentary section, in addition to the oceanic crustal basement, are affected by this fault system (Gulf of Suez trend).

b. A minor NE-SW trend of cross faults exist. This trend is believed to be of shallower and younger origin and of relatively smaller effect on the shallow sedimentary section than the NW-SE trend.

c. The older NW-SE trend dissects the oceanic crust into blocks interacting together to form some like horsts and grabens which affect the shallow sedimentary section.

Concerning the Two-Dimensional Models

The highest goodnesses of fit obtained are 0.834 and 0.848 for the resulting two models (Fig. 10 and 11) representing the profiles C_4 E_2 and C_3 D_3 respectively. The corresponding correlation coefficients are 0.913 and 0.921, respectively.

The study and investigation of both models show that each model is composed of four sedimentary bodies covered, with sea water and is affected by the above mentioned probably structural changes. The corresponding densities are adjusted to, from bottom to top, 2.545×10^{-3}, 2.655×10^{-3}, 2.975×10^{-3}, and 2.645×10^{3} kg.m^{-3}. The results show that the normal fault systems (F_1, F_2, F_3 and F_4) are confirmed to affect the whole study area and to strike along the Red Sea clysmic trend. Another

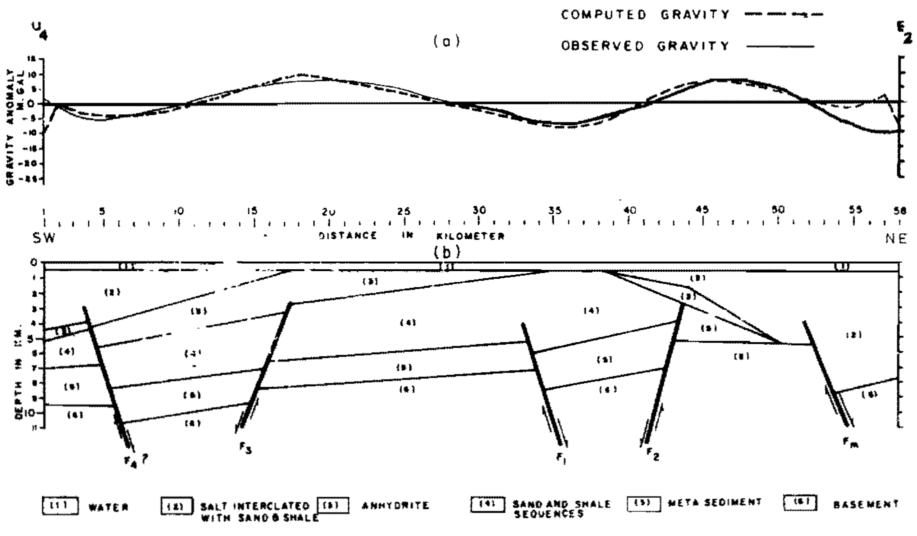

FIG. 10. Computed and observed gravity anomalies (a) along C_4 E_2 profile and the corresponding assumed structural model (b).

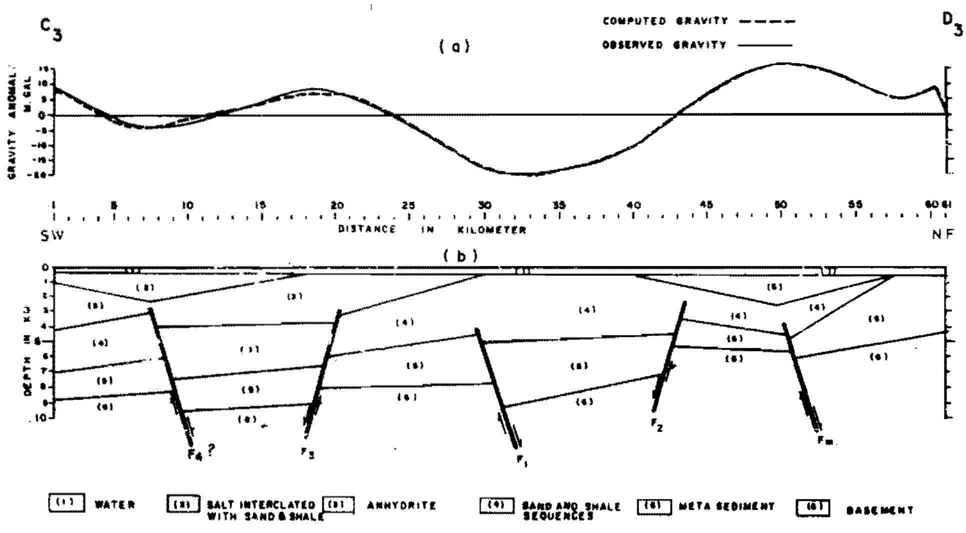

FIG. 11. Computed and observed gravity anomalies (a) along C_3 D_3 profile and the corresponding assumed structural model (b).

fault Fm is assumed to exist in the model rather than in the gravity map. The existing normal faulting, in a closely parallel system of a dissection manner, may clarify the rifting effect of Red Sea. The existence of oceanic Gabbro within the NE-extreme of C_4 E_2 profile at a relatively shallow depth (5 km), as evidenced in Qusier Blx-well and indicated by the horstal belt DD' (Fig. 2 and 8).

On a regional scale, the whole structural model fits into and satisfies the monoclinal feature which could be exhibited from the regional gravity map (Fig. 5). The general trend of the basement surface's attitude is trending to dip towards the western side of the study area. This tendency may explain the thinning of the continental crust eastward.

From a comparative quantitative analysis of the seismic section, from Sp. 16-E to Sp. 233-W, and the nearby gravity model C_4 E_2, concerning the basement average depth and the fault displacements as determined for some structures, the following tabulated results are obtained :

Belt	Depth (km)	
	Seismic section	Gravity model
$A'A$	7.7	7.7
$B'B$	7.8	7.5
$C'C$	5.0	5.2
$D'D$	7.2	7.8

Fault	Displacement (km)	
	Seismic section	Gravity model
F_1	1.0	1.2
F_1	1.6	1.7
F_m	3.0	3.1

The slight discrepancies between seismic and gravity results are probably due to the end effect of the model (Grant and West 1965). Stratigraphic correlation between the seismic section and the model shows that four common layers, rather than sea water are overlying the basement. These layers are (from bottom to top): metasediments, sand and shale sequences of Kareem-Rudeis formation, anhydrite, and salt intercalated with sand and shale streaks. The two bottom layers overlying the basement are wedged to the East of fault plane F_2 in both seismic section and gravity models. Dealing with hydrocarbon potentiality expectation, it would be confined to the sand/shale sequences of Kareem-Rudeis formation, particularly on the upthrown sides of F_3 and F_4 fault planes. This is due to the favorable thick sedimentary section at these locations.

Acknowledgement

The authors are deeply indebted to Dr. Al El-Saharty, Professor of Geophysics, University of Alexandria for his kind supervision and valuable guidances throughout this work.

References

Ajakaiye, D.E. and **Awad, M.B.** (1982) A Gravity Study of the Shira Younger Granite Ring Complex, Nigeria, *18th Ann. Conf. Nig. Min. Geosc. Soc.*, Kaduna Sess 58.

Barker, H. and **Schoell, M.** (1972) New deeps with brine and metalliferous sediments in the Red Sea, *Nature, Phys. Sci.* **240:** 153-158.

Bott, M.H.P. and **Smith, R.A.** (1958) The estimation of the limiting depth of gravitating bodies, *Geoph. Prosp.* **6:** 1-10.

Darke, C.L. and **Girdler, R.W.** (1964) A geophysical study of the Red Sea. *Geoph. J. Roy. Ast. Soc.* **8:** 473-495.

Davis, J.C. (1973) *Statistics and Data Analysis in Geology*, John Willey & Sons, Inc., New York, p. 549.

Grant, F.S. and **West, G.F.** (1965) *Interpretation Theory in Applied Geophysics.* McGraw-Hill Inc., Toronto, p. 584.

Hubbert, M.K. (1948) A line integral method of computing the gravimetric of two dimensional masses, *Geoph.* **14:** 517-534.

Kabbani, F.K. (1970) *Geophysical and structural aspects of the central Red Sea rift valley. Royal Soc. London Philos. Trans. V.A.* **267:** 89-97.

Lowell, J.D. and **Genik, G.J.** (1972) Sea floor spreading and structural evaluation of the southern Red Sea, *AAPG Bull.* **5612:** 247-259.

Nagy, D. (1974) *The Gravitational Effect of Two-Dimensional Masses of Arbitrary Cross-Section,* Pub. Grav. Div. of Ottawa, Canada.

Rosenbach, O. (1953). A contribution to computation of second derivative from gravity data, *Geoph.* **18:** 894-912.

Rosser, A.H. (1975) A detailed magnetic survey of southern Red Sea, *Geol., Jb. D.* **13:** 131-153.

Talwani, N. and **Reirtzler, J.** (1964). Computation of potential anomalies caused by two-dimensional structures of arbitrary shape, *In:* **Parks, G.A. (Ed.)** *Computers in Mineral Industries Standard.*

Telford, W.R., Geldart, L.P., Sheriff, R.E. and **Keys, D.A.** (1976) *Applied Geophysics,* Cambridge Univ. Press, p. 860.

تفسير المشاهدات التثاقلية في منطقة القصير – مرسى علم ، البحر الأحمر ، مصر

مراد عوض ، ياقوت العبد و عزت الحاج
المعهد القومي لعلوم البحار ، الاسكندرية – مصر ؛ كلية العلوم ، جامعة الاسكندرية – مصر
و شركة بترول الصحراء الغربية ، الاسكندرية – مصر

المستخلص . يهدف البحث إلى تقييم الوضع الجيولوجي لطبقات ما تحت السطح في منطقة القصير – مرسى علم البحرية – بالبحر الأحمر ، وذلك لاستكشاف وجود الهيدروكربونات في المنطقة . وفي ضوء المعلومات المستمدة من خريطة بوجير التثاقلية وقطاع سيزميٍّ وبئرين محفورتين بالمنطقة ، تم إعداد خرائط كنتورية للشاذات النطاقية والمحلية والمشتقة التفاضلية الرأسية الثانية . وقد أدى التفسير الكيفي والكمي لهذه الخرائط مع القطاع السيزمي إلى عمل خريطة للتراكيب الجيولوجية في طبقات القطاع الرسوبي ، وتأثرها بالفوالق . كما تم حساب نموذجين ثنائيي الأبعاد لهذه التراكيب على طول قطاعين يمران بالمنطقة .

وتشير النتائج إلى أن المنطقة تعاني ن التمزق والانتشار القاري استدلالاً بوجود نظامين من الفوالق العميقة والمتوازية ، أحدهما يمتد من الشمال الغربي إلى الجنوب الشرقي موازيا للبحر الأحمر ، والآخر يمتد عموديا عليه – وأن التركيب العام للمنطقة عبارة عن طيَّه محدبة ذات محور شمال شرق شرق / جنوب غرب غرب يحتوى على تراكيب من المصاطب والأحواض ، وإلى احتمال وجود الهيدروكربونات في الأجزاء السميكة من طبقة «كريم – رودس» عند بعض الفوالق .